Paper for the ASME 6th International Power Transmission and Gearing Conference, September 1992

Computational Issues Associated With Gear Rattle Analysis Part I : Problem Formulation

C. Padmanabhan, T. E. Rook
Graduate Research Associates

R. Singh
Professor

Department of Mechanical Engineering
The Ohio State University
Columbus, Ohio 43210-1107

Summary

This paper proposes a new procedure for formulating the gear rattle type problem analytically before attempting a numerical solution. This step is necessary due to the nature of the mathematical formulation with vibro-impacts, which is non-analytical and hence causes numerical "stiffness". The procedure is essentially an "intelligent" pre-processing stage and is based on our vast experience in simulating such systems. Important concepts such as order reduction, gear contact ratio, appropriate choice of non-dimensionalization parameters are illustrated through several examples.

1. Introduction

Gear backlash induce vibro-impacts have been studied by using a variety of techniques such as digital simulation (Sakai et al., 1981; Ohnuma et al., 1985; Singh et al., 1989; Chikatani and Suehiro, 1991; Weidner and Lechner, 1991), analog simulation (Veluswami and Crossley, 1975; Comparin and Singh, 1990), quasi-steady state analysis (Seaman et al., 1984), multi-body approach (Pfeiffer and Kunert, 1990) and experimental noise perception(Croker et al., 1990; Rust et al., 1990; Johnson and Hirami, 1991). Most of the studies have focused on the rattle phenomena in automotive manual transmissions. A number of research issues still remain unresolved (Singh et al., 1989; Pfeiffer and Kunert, 1990). Numerical solutions issue, the focus of this paper, is one typical example of such research problems which are of interest both from academic and practical viewpoints.

Consider the example case of an automotive transmission. Multiple clearance nonlinearities associated with backlash between gears, multi-staged clutches or dampers, dual mass flywheel, spline or synchronizer backlash and bearing clearances are typically encountered in a given problem. Obviously, one should attempt to model the complete transmission system, however the dimension of analysis is usually too large. Accordingly reduced order models must be pursued (Singh et al., 1989; Comparin and Singh, 1990). Several investigators have even examined only the flywheel-clutch system. Whether such a reduced order model is appropriate, it is difficult to assess apriori.

Since the number of degrees of freedom involved is fairly large, numerical simulation of the deterministic system is often the preferred method of solution. However, some of the earlier investigations (Singh et al., 1989; Croker et al., 1990; Padmanabhan, 1990) have reported numerical difficulties in the direct time domain integration process. These are directly related to the nature of the vibro-impact model which is non-analytic. The periodic occurrence of impacts causes high frequency transients resulting in rapid reduction in step sizes. In addition, the ratio of the largest (in magnitude) to the smallest (non-zero) eigenvalue of the system matrix may become very large causing an ill-conditioning of the system matrix. These two phenomena cause the system to be characterized as "stiff" according to the computational literature (Aiken, 1985; Miranker, 1981), even though there is debate regarding the true meaning of "stiff" problems (Aiken, 1985).

2. Scope and Objectives

This paper proposes a procedure for formulating the problem analytically before the governing equations are solved numerically. The process outlined is iterative in nature and it reduces some of the difficulties faced in vibro-impact system analyses. This procedure can be characterized as an "intelligent" pre-processing stage and is followed by the solution and/or the post-processing stage. Figure 1 shows a flowchart of the proposed problem solving procedure; it is based on our vast experience with many simulations of gear rattle type problems.

In the first part of this series of two papers the various issues related to the pre-processing stage are discussed in detail and key concepts are demonstrated through several examples. The companion paper (Part II) establishes evaluation criteria for solution algorithms. Several well known and commercially available numerical algorithms are used to simulate rattle problems and the results are critically compared in order to identify specific computational problems and to seek reasonably accurate and reliable solutions.

The first step is to examine the eigensolutions of the overall transmission system within the frequency range of interest. The nonlinear dynamic model can be linearized around an operating point and the corresponding linear model can be used to reduce the order or dimension of the model through appropriate lumping of various inertias. Next, a suitable non-linear model is developed and the governing equations of motion are written and then non-dimensionalized.

To understand the importance of "stiff" problems a linearized

contact ratio analysis (to be explained in section 7) based on the time-averaged gear mesh stiffness and/or clutch stiffness is carried out. Such an analysis provides insight on the severity of the possible ill-conditioning which is then used to adjust the non-dimensionalizing parameters in order to reduce or avoid computational problems during the course of numerical integration. None of these issues have been addressed by prior investigators.

3. Selection of System Dimension

As an example consider a hypothetical, yet reasonable eight degree-of-freedom torsional model of an automotive transmission with three gear pairs, a flywheel and a clutch as shown in Figure 2. Initially all the torsional springs are assumed to be linear and the undamped system is solved for the natural frequencies ω_r and the corresponding modeshapes or eigenvectors ψ_r, where r=1, 2,..8. Figure 3 shows the first three non-rigid body modes and Table 1 lists all of the ω_r values. The excitation for such a system is usually of the form $T_e(t) = \sum_{j=1}^{n} T_{aj} \sin(j\Omega_e t)$ and is due to rotating mass unbalances and/or prime mover torque pulsations. The important excitation frequencies typically lie in the low frequency range say 25-75 Hz. As can be seen from Figure 3, for this range of excitation frequencies the linear system response is dominated by the first mode (22 Hz) with a much smaller participation of the second mode. In each mode of vibration however, it is observed that there is no or little relative motion between the gear pairs. Based on this information one can then lump the second and third gears on the countershaft onto their conjugate parts on the mainshaft. Further one can lump the final two gears on the mainshaft onto the first gear, thus reducing the original eight degree-of-freedom system into a four degree-of-freedom model. The inertia at station 3 is replaced by $I_3=I_3+I_5+I_7+I_6(R_5/R_6)^2+I_8(R_7/R_8)^2$. At the end of this stage, the non-linear model can be developed.

Table 1. The natural frequencies ω_r, in rad/s of
(a). the eight degree-of-freedom system shown in Figure 2
(b). the reduced four degree-of-freedom system in Figure 4.

(a).

ω_1	ω_2	ω_3	ω_4	ω_5	ω_6	ω_7	ω_8
0.0	346.0	7412	10134	18526	48442	50869	68632

(b).

ω_1	ω_2	ω_3	ω_4
0.0	346.0	7937.0	48091

4. Development of a Nonlinear Model

The following non-linearities are introduced in the four degree-of-freedom model developed; it is now shown in Figure 4.
(a). A multi-stage clutch stiffness between the flywheel (number one) and clutch (number two) inertias.
(b). A clearance nonlinearity between clutch (number two) and input gear (number three) inertias.
(c). A backlash between the gear number three and four.
The governing equations of motion are as follows

$$\bar{I}_1\ddot{\bar{\theta}}_1 + \bar{T}_{12} + \bar{T}_{d1} = \bar{T}_{e1}(t) \tag{1}$$

$$\bar{I}_2\ddot{\bar{\theta}}_2 - \bar{T}_{12} + \bar{T}_{23} + \bar{T}_{d2} = \bar{T}_{e2}(t) \tag{2}$$

$$\bar{I}_3\ddot{\bar{\theta}}_3 - \bar{T}_{23} + \bar{R}_3\bar{F}_{34} + \bar{T}_{d3} = \bar{T}_{e3}(t) \tag{3}$$

$$\bar{I}_4\ddot{\bar{\theta}}_4 - \bar{R}_4\bar{F}_{34} + \bar{T}_{d4} = \bar{T}_{e4}(t) \tag{4}$$

with constraint torques $\bar{T}_{12}$, $\bar{T}_{23}$, force $\bar{F}_{34}$ and drag torques $\bar{T}_{di}$ defined as

$$\bar{T}_{12} = \bar{C}_1 g(\bar{\delta}_1)\dot{\bar{\delta}}_1 + \bar{K}_1 \bar{f}(\bar{\delta}_1); \quad \bar{T}_{23} = \bar{C}_2 g(\bar{\delta}_2)\dot{\bar{\delta}}_2 + \bar{K}_2 \bar{f}(\bar{\delta}_2) \tag{5, 6}$$

$$\bar{F}_{34} = \bar{C}_3 g(\bar{\delta}_3)\dot{\bar{\delta}}_3 + \bar{K}_3 \bar{f}(\bar{\delta}_3); \quad \bar{T}_{di} = \bar{D}_{mi}\dot{\bar{\theta}}_{mi} + \bar{D}_{ai}\dot{\bar{\theta}}_{ai} \tag{7, 8}$$

$$\bar{\delta}_1 = \bar{\theta}_1 - \bar{\theta}_2; \quad \bar{\delta}_2 = \bar{\theta}_2 - \bar{\theta}_3; \quad \bar{\delta}_3 = \bar{R}_3\bar{\theta}_3 - \bar{R}_4\bar{\theta}_4 \tag{9-11}$$

Also the excitation terms are defined as follows

$$\bar{T}_{ei}(t) = \bar{T}_{mi} + \bar{T}_{ai}(t); \quad \bar{T}_{ai}(t) = \sum_j \bar{T}_{a_{ij}} \sin(j\Omega_e t) \tag{12, 13}$$

The clearance type non-linear elements, shown in Figure 5, can be related to the clutch torque characteristics or gear/spline backlash and are defined as

$$\bar{f}(\bar{\delta}_i) = \begin{cases} \bar{\delta}_i - (1-\alpha_i)\bar{b}_i, & \bar{b}_i < \bar{\delta}_i \\ \alpha_i\bar{\delta}_i \quad , & -\bar{b}_i \le \bar{\delta}_i \le \bar{b}_i \\ \bar{\delta}_i + (1-\alpha_i)\bar{b}_i, & \bar{\delta}_i < -\bar{b}_i \end{cases} \tag{14}$$

$$g(\bar{\delta}_i) = \begin{cases} 1.0, & \bar{b}_i < \bar{\delta}_i \\ \beta_i \, , & -\bar{b}_i \le \bar{\delta}_i \le \bar{b}_i \\ 1.0, & \bar{\delta}_i < -\bar{b}_i \end{cases} \tag{15}$$

5. Non-Dimensionalization

The equations of motion can be written in a non-dimensional form by defining $t = \bar{\omega}\bar{t}$, $\theta_i = \bar{\theta}_i/\bar{\psi}_c$, $\bar{\psi}_c = \bar{x}_c/\bar{R}_c$ where $\bar{\omega}, \bar{\psi}_c, \bar{x}_c, \bar{R}_c$ represent characteristic frequency, angular displacement, length and radius respectively. The purpose of this procedure is two-fold. The first one is to reduce the number of system parameters and variables involved, and the second purpose is to possess a capability to adjust key parameters in such a manner which may reduce the ill-conditioning of the system matrices during numerical integration. Ill-conditioning occurs due to the presence of components in the solution whose frequency ratio is large. Then Equations 1-4 become

$$\theta_1'' + \eta_{11}g(\delta_1)\delta_1' + \Omega_{11}^2 f(\delta_1) - \xi_{11}\theta_1' = T_{e_1}(t) \tag{16}$$

$$\theta_2'' + \eta_{22}g(\delta_2)\delta_2' - \eta_{12}g(\delta_1)\delta_1' + \Omega_{22}^2 f(\delta_2) - \Omega_{12}^2 f(\delta_1) - \Omega_{12}^2 f(\delta_1) - \xi_{22}\theta_2' = T_{e_2}(t) \tag{17}$$

$$\theta_3'' + \eta_{33}g(\delta_3)\delta_3' - \eta_{23}g(\delta_2)\delta_2' + \Omega_{33}^2 f(\delta_3) - \Omega_{23}^2 f(\delta_2) - \xi_{33}\theta_3' = T_{e_3}(t) \tag{18}$$

$$\theta_4'' - \eta_{34}g(\delta_3)\delta_3' - \Omega_{34}^2 f(\delta_3) - \xi_{44}\theta_4' = T_{e_4}(t) \tag{19}$$

Here individual terms are defined as:

$$\xi_{ii} = \frac{\bar{D}_i}{\bar{I}_i\bar{\omega}} \tag{20}$$

$$\eta_{ij} = \frac{\bar{C}_i}{\bar{I}_j\bar{\omega}},\ i = 1,2;\quad j = 1,2,3;\quad \eta_{3k} = \frac{\bar{R}_c\bar{R}_k\bar{C}_3}{\bar{I}_k\bar{\omega}},\ k = 3,4; \quad (21, 22)$$

$$\Omega_{ij}^2 = \frac{\bar{K}_i}{\bar{I}_j\bar{\omega}^2},\ i = 1,2;\ j = 1,2,3;\ \Omega_{3k}^2 = \frac{\bar{R}_c\bar{R}_k\bar{K}_3}{\bar{I}_k\bar{\omega}^2},\ k = 3,4; \quad (23, 24)$$

$$T_{e_i}(t) = \frac{\bar{T}_{m_i} + \bar{T}_{a_i}(t)}{\bar{I}_i\bar{\omega}^2\bar{\psi}_c},\quad \bar{T}_{a_i}(t) = \sum_j \bar{T}_{a_{ij}}\sin(\Omega_{e_{ij}}t), \quad (25, 26)$$

$$e(t) = \varepsilon\sin(N\Omega_{e_{11}}t) \quad (27)$$

$$\Omega_{e_{ij}} = j\frac{\bar{\Omega}_{e_i}}{\bar{\omega}},\quad i = 1,\ldots,4;\quad j = 1,2,\ldots; \quad (28)$$

$$\bar{\psi}_c = \frac{\bar{x}_c}{\bar{R}_c},\quad \theta_i = \frac{\bar{\theta}_i}{\bar{\psi}_c} \quad (29, 30)$$

In the next section the concept of contact ratio is introduced, which is used to demonstrate the effectiveness of non-dimensional formulation in reducing ill-conditioning of system matrices.

6. Numerical Stiffness Issue

The equations developed in section 5 can be written in the vector form as $dy/dt=p(y,t)$. Most numerical codes linearize around an operating point y_0, hence we have the following expression where the higher order terms are ignored: $p(y,t) \equiv p(y_0,t) + [J](y - y_0)$, where $[J]=dp/dy$ is the Jacobian matrix evaluated at y_0. The local eigenvalues of the Jacobian is used to define numerical "stiffness". Aiken (1985), who classifies the vibro-impact problem as stubborn due to system discontinuities, re-occuring mechanical or physical stiffness and the possibility of the existence of highly oscillatory components, defines numerical stiff categories based on R_λ, the ratio of the largest eigenvalue (in magnitude) to the smallest non-zero eigenvalue:

Mildly stiff	$R_\lambda < 10^2$
Strongly stiff	$10^3 < R_\lambda < 10^5$
Extremely stiff	$10^6 < R_\lambda < 10^8$
Pathologically stiff	$10^9 < R_\lambda$

Hairer and Wanner (1991) evaluate numerical stiffness in terms of the magnitude of the largest eigenvalue. Numerical stiffness occurs when the product of the dominant eigenvalue and the step size lies on the border of the stability domain of the numerical algorithm.

In order to estimate R_λ and/or the largest eigenvalue the concept of contact ratio Γ is introduced. The idea behind this procedure is to replace the time dependent Jacobian components (essentially the non-linear elements) by a time-averaged value. When such a linearization is done the eigenvalues of the Jacobian correspond to the eigenvalues of the physical model itself. This is explained by using the gear pair as an example. If two gears are connected by a backlash element the pair may become physically uncoupled. A loss of contact can be due to an alternating load, light mean load and/or a combination of both. Hence, a linear effective stiffness based on the time the pair is uncoupled can be defined. The fraction of the time the pair is uncoupled defines the contact ratio Γ. For instance if the gears are in the backlash region 50% of the time then Γ=0.5.

The contact ratio, Γ, may be estimated in one of the following ways:

(1). By using the cross and auto spectral densities to estimate the transfer function from which the dynamic stiffness may be obtained. See Bendat and Piersol (1986) for typical signal processing issues.

(2). By keeping track of the time history of $f(\delta)$ which is a square wave bounded between zero and one; it may not be periodic depending on the nature of the nonlinearities. Then Γ may be found by time averaging the signal i.e., $\Gamma=(1/N)\Sigma|\delta(t_m)|$ and is between 0 and 1.

(3). By using the describing function or harmonic balance method (Gelb and Vander Velde 1968; Comparin and Singh 1989) to analytically approximate the value of Γ. This method has the benefit that if one has a prior knowledge of the expected amplitude of motion, the contact ratio can be obtained without any numerical simulations. Figure 6 shows the three types of impacts possible, and Figure 7 shows typical Γ values for the single-sided and double-sided impact cases. As can be seen from these results, an increase in the amplitude of single-sided impacts means more time is being spent in the backlash region thus reducing Γ. For the double-sided case, a very large amplitude results in a saturation effect pushing Γ towards one. See Rook (1992) for further details.

7. Results using Contact Ratio Concept

The concept of contact ratio is now used in the four degree-of-freedom model developed earlier and the function $f(\delta_1)$ is replaced by $\Gamma_c\delta_1$ and the function $f(\delta_3)$ is replaced by $\Gamma_g\delta_3$, where $0<\Gamma_c<1$ and $0<\Gamma_g<1$ (in equations 1-4 and 16-19). The $f(\delta_2)$ is assumed to be δ_2 (linear) and the modified system's natural frequencies (undamped) are evaluated. Equations 1-4 and 16-19 have all the variables in the torsional form. One could instead consider a mixed form, for instance, replacing θ_3 by $x_3=R_3\theta_3$ and θ_4 by $x_4=R_4\theta_4$. This form has two torsional variables and two translational variables. The mixed formulation (non-dimensional) is effective in reducing ill-conditioning when compared to a pure torsional or translational formulation. In fact the pure torsional or translational non-dimensional formulation gives the same R_λ as the corresponding dimensional formulation. Hence all the subsequent results use a mixed formulation. Figures 8 and 9 show a plot of the three non-rigid body frequencies as Γ_g is varied for Γ_c=1.0 and 0.10 respectively. The dimensional form is plotted in Figures 8a and 9a while the non-dimensional form is plotted in Figures 8b and 9b. Figure 10 illustrates a variation in R_λ as Γ_g is varied. It is observed from the results the stiffness ratio is indeed lower for the non-dimensional case. Actual numerical integrations (though not included here) confirms these trends. This demonstrates the effectiveness of the non-dimensional formulation in reducing or avoiding ill-conditioning. This is clearly seen from Figure 8b where in the dimensional case the highest R_λ value is about seventy which implies that we have components in the solution which have a frequency ratio of at least seventy. Conversely the non-dimensional value barely reaches twenty. This definitely improves the computational efficiency. The study also shows that at low contact ratios (associated with light mean loads and/or high alternating loads) the natural frequencies are much closer than at high contact ratios. Depending upon Γ significant changes in the non-linear behavior are seen as evident by actual numerical integrations.

Another example case is considered by introducing damping in the system. The poles (complex eigenvalues) are examined for a system with only a gear backlash nonlinearity. The clutch and the intermediate shaft are assumed to be linear, which implies that while $f(\delta_3)=\Gamma_g\delta_3$, $f(\delta_1)=\delta_1$, and $f(\delta_2)=\delta_2$. Figure 11 shows a variation of the undamped natural frequencies ω_3 and ω_4 as a

function of Γ_g. The behavior of the poles for the corresponding damped system (viscous damping) is shown in Figure 12. The third and fourth poles of the system come close to each other at about Γ_g =0.50. Figure 12a shows their variation for $0.1<\Gamma_g<1.0$. Similarly the second and third poles come very close to each other at very low Γ_g (See Figure 12b). Based on these results strong nonlinear behavior is anticipated at low loads, which is confirmed by actual time integration. The companion paper includes results of time integration for this case (termed model 3A).

8. Concluding Remarks

The entire problem formulation and pre-processing process described in this paper is iterative in nature and discretion or caution must be exercised at each stage. It must be completed in order to generate a suitable set of non-linear ordinary differential equations. This study is used to detect trends which could cause significant numerical problems or changes in dynamic response. At the end of this process a suitable algorithm must be selected by the user which is then utilized to carry out simulation studies of the system. The evaluation criteria for algorithms forms the basis of the companion paper.

Issues which are being currently considered include alternate forms for the clearance type stiffness and damping nonlinearities, in terms of continuous and well behaved analytical functions. Also the formulation of the governing equations in terms of relative displacements has been attempted. Although this has the distinct advantage of reducing the number of degrees-of-freedom by one as compared to an absolute variable formulation, however absolute variables like accelerations, velocities or displacements cannot be recovered numerically.

Acknowledgment

We wish to acknowledge the Nissan Technical Center (Japan) and the Center for Automotive Research at the Ohio State University for supporting this research.

References

Aiken, R. C., 1985, "Classification of other "stubborn" problem types," *Stiff Computation*, Aiken, R. C., ed., Oxford University Press, New York, pp. 16-21.

Bendat, J. S., and Piersol, A. G., 1986, "*Random Data: Analysis and Measurement Procedures*," Second edition, John Wiley and Sons, New York.

Chikatani, Y., and Suehiro, A., 1991, "Reduction of Idling Rattle Noise in Trucks," SAE Paper No. 911044, pp. 49-56.

Comparin, R. J., and Singh, R., 1989, "Frequency response characteristics of an Impact Pair," *Journal of Sound and Vibration*, vol. 134, pp. 259-290.

Comparin, R. J., and Singh, R., 1990, "Frequency Response of Multi-Degree-of-Freedom Systems with Clearances," *Journal of Sound and Vibration*, vol. 142, pp. 101-124.

Croker, M. D., March, J. P., and Greer, R. J., 1990, "Transmission Rattle Analysis," *Proceedings of IMechE, First International Conference on Gearbox Noise and Vibration*, C404/005, pp. 121-127.

Gelb, A., and Vander Velde, W. E., 1968, "*Multiple-Input Describing Functions and Nonlinear System Design*," McGraw-Hill, New York.

Hairer, E., and Wanner, G., 1991, "*Solving Ordinary Differential Equations II: Stiff and Differential-Algebraic Problems*," Springer-Verlag, Berlin.

Johnson,O., and Hirami, N., 1991, "Diagnosis and Objective Evaluation of Gear Rattle," SAE Paper No. 911082, pp. 381-396.

Miranker, W. L., 1981, "*Numerical Methods for Stiff Equations*," D. Reidel Publishing Company, Boston.

Ohnuma, S., Yahata, S., Inagawa, M., and Fujimoto, T., 1985, "Research on Idling Rattle of Manual Transmission," SAE Paper No. 850979, pp. 159-167.

Pfeiffer, F., and Kunert, A., 1990, "Rattling Models from Deterministic to Stochastic Processes," *Nonlinear Dynamics*, vol. 1, pp. 63-74.

Padmanabhan, C., 1990, "Dynamic Analysis of Clearance Nonlinearities in Automotive Systems," M. S. Thesis, The Ohio State University, Columbus, Ohio.

Rook, T. E., 1992, "Nonlinear dynamic analysis of a reverse idler gear pair," M. S. Thesis, The Ohio State University, Columbus, Ohio.

Rust, A., Brandl, F. K., and Thien,G.K., 1990, "Investigations into gear rattle phenomena- key parameters and their influence on gearbox noise," *Proceedings of IMechE, First International Conference on Gearbox Noise and Vibration*, C404/001, pp. 113-120.

Sakai, T., Doi, Y., Yamamoto, K., Ogasawara, T., and Narita, M., 1981, "Theoretical and Experimental Analysis of Rattling Noise of Automotive Gearbox," SAE Paper No. 810773, pp. 1-10.

Seaman, R. L., Johnson, C. E., and Hamilton, R. F., 1984, "Component Inertial effects on Transmission Design," SAE Paper No. 841686, pp. 1-19.

Veluswami, M. A., and Crossley, F. R. E., 1975, "Multiple Impacts of a Ball between two Plates, Part 1: Some Experimental Observations," ASME *Journal of Engineering for Industry*, vol. 97, pp. 820-827.

Weidner, G., and Lechner, G., 1991, "Rattling Vibrations in Automotive Transmissions," *Proceedings, JSME International Conference on Motion and Power Transmissions*, Hiroshima, Japan, pp. 37-42.

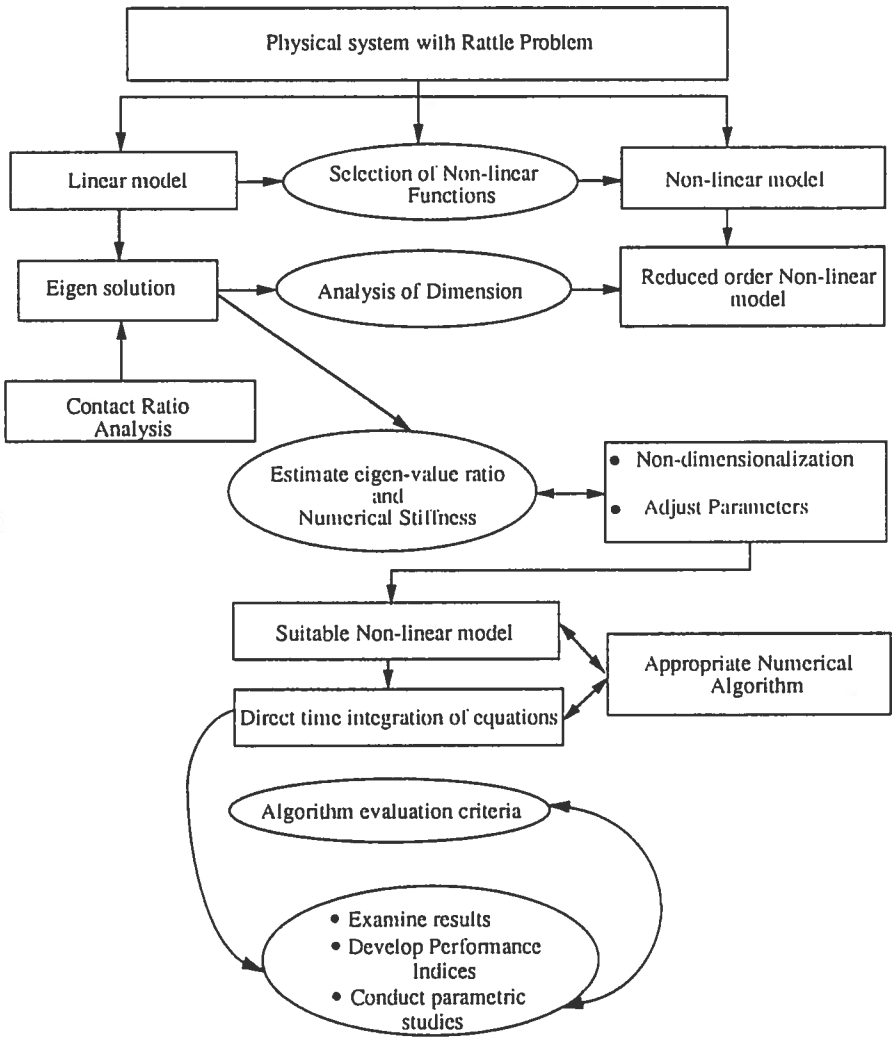

Figure 1. The proposed procedure for solving rattle type problems

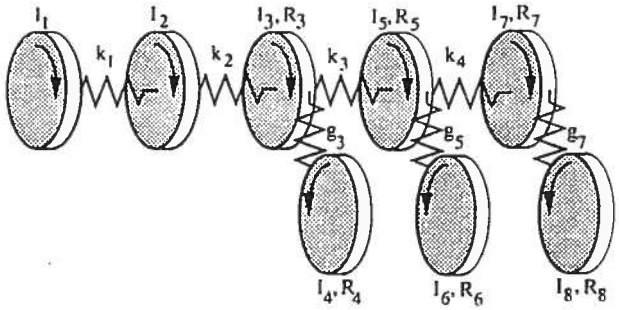

Figure 2. An eight-degree-of-freedom torsional model of an automotive transmission.

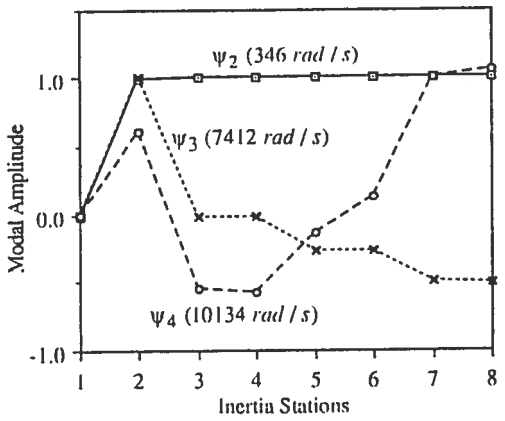

Figure 3. The first three non-rigid body modes, ψ_2, ψ_3 and ψ_4, of the torsional system shown in Figure 2.

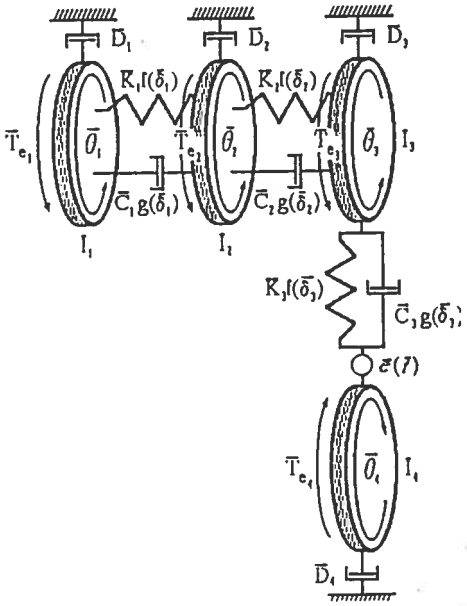

Figure 4. Generic multi-degree-of-freedom torsional geared system with multiple clearance non-linearities.

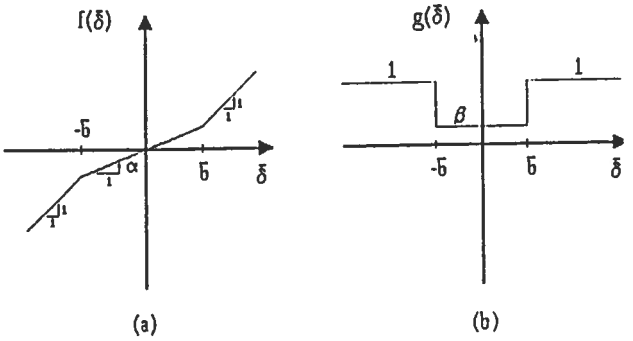

Figure 5. (a). Clearance type stiffness non-linearity and (b). Clearance type damping non-linearity.

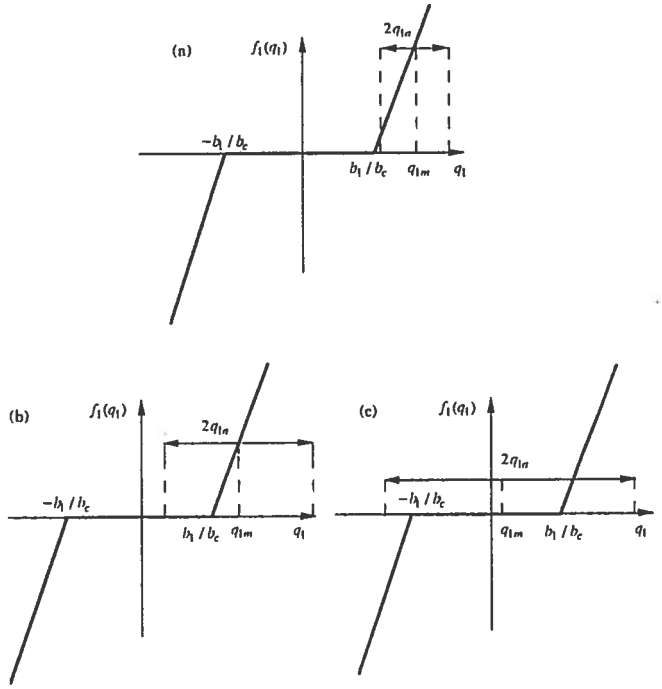

Figure 6. Different vibro-impact regimes: (a). no-impact, (b). single-sided and (c). double-sided vibro-impacts.

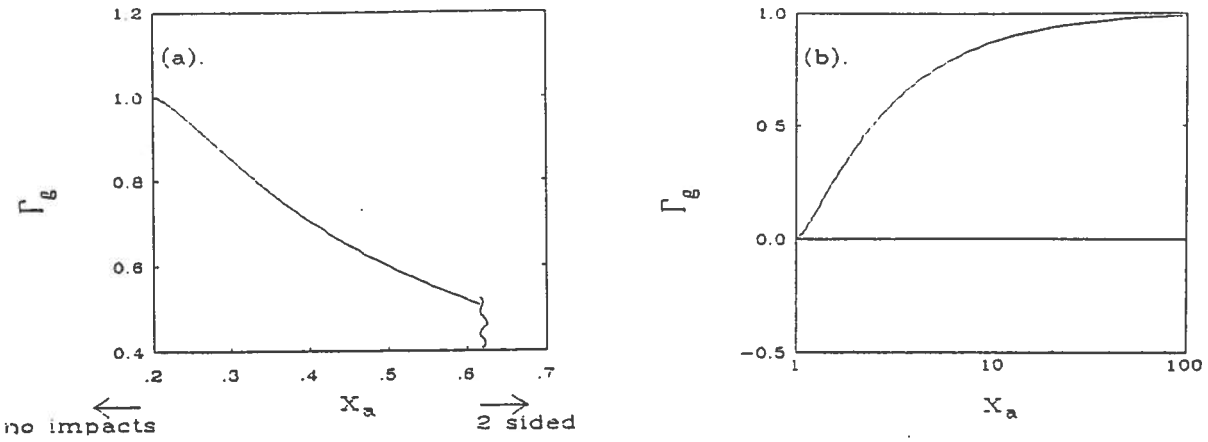

Figure 7. The variation of Γ_g with the response amplitude x_a, for (a). single-sided impacts, and (b). double-sided impacts.

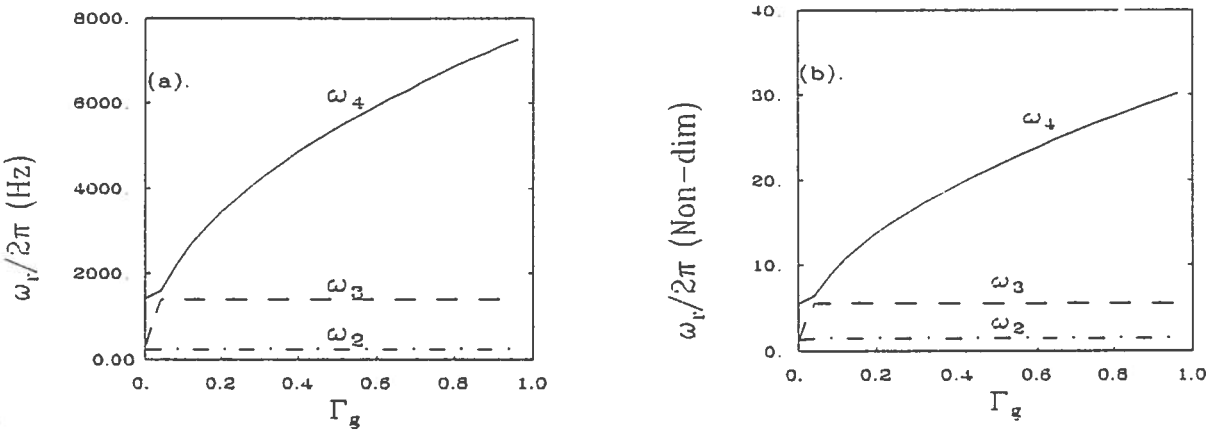

Figure 8. The changes in ω_r of the four degree-of-freedom system, shown in Figure 4, for $\Gamma_c = 1.0$: (a). Dimensional case, and (b). Non-dimensional case.

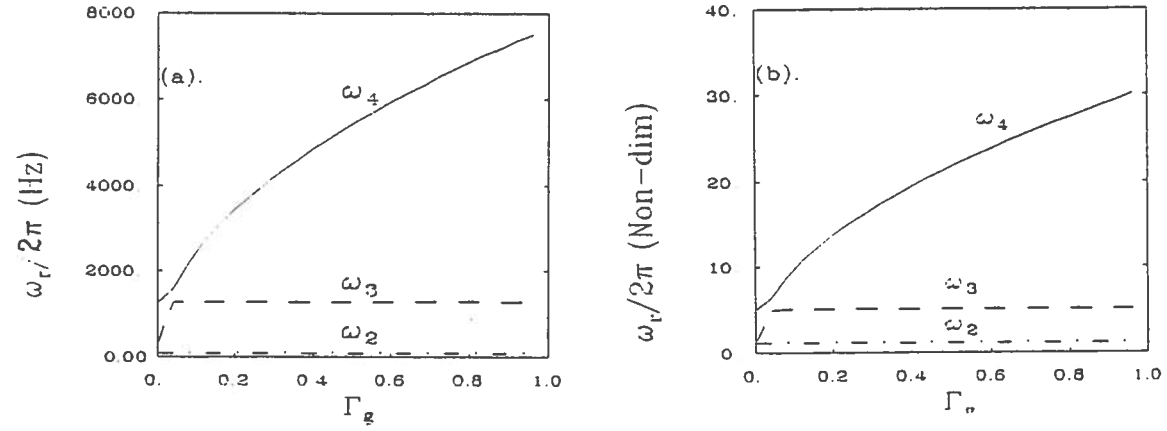

Figure 9. The changes in ω_r of the four degree-of-freedom system, shown in Figure 4, for $\Gamma_c = 0.10$: (a). Dimensional case, and (b). Non-dimensional case.

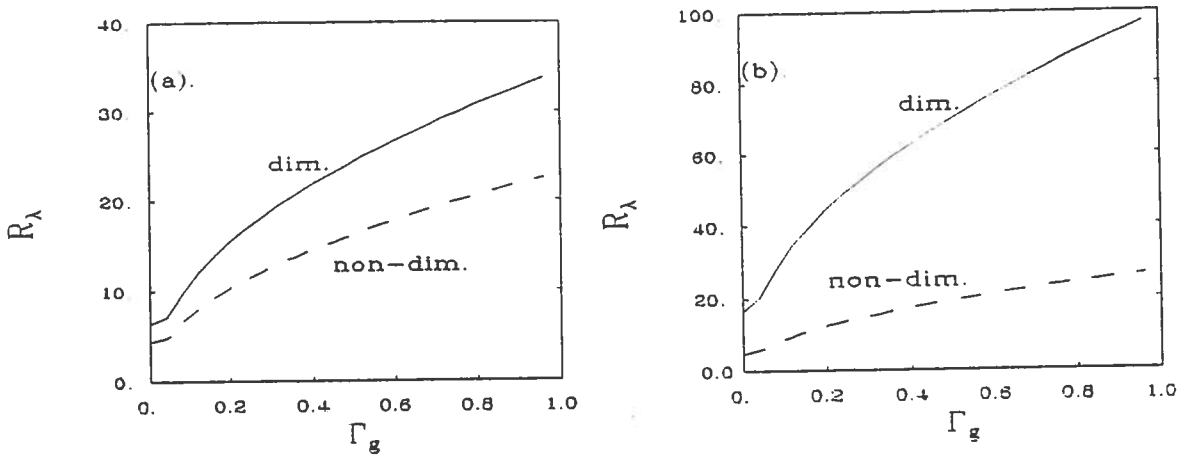

Figure 10. Variation of R_λ with Γ_g for (a). $\Gamma_c = 1.0$, and (b). $\Gamma_c = 0.10$.

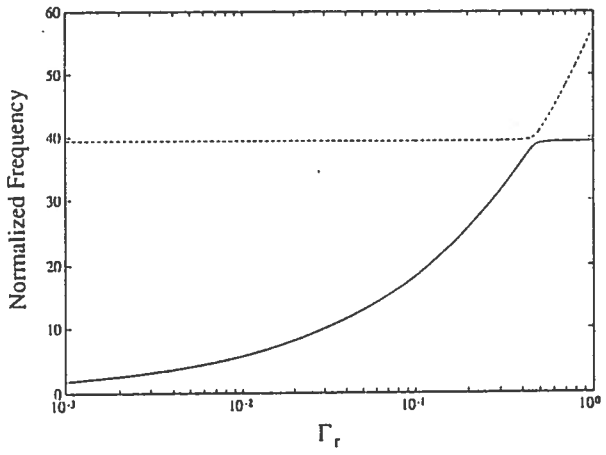

Figure 11. Variation of the undamped natural frequencies with contact ratio, Γ_r. ——, ω_3; ----, ω_4.

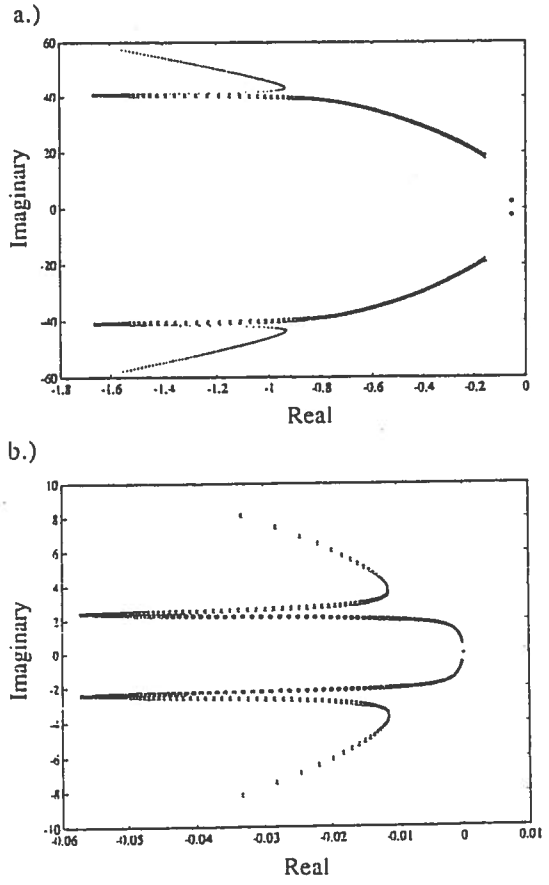

Figure 12. Variation of eigenvalues with contact ratio, Γ_r
(a). $0.1 \le \Gamma_r \le 1.0$, spectral coupling between modes 3 and 4.
(b). $10^{-4} \le \Gamma_r \le 0.01$, spectral coupling between modes 2 and 3.
000 γ_2, γ_2^*; xxx γ_3, γ_3^*; .... γ_4, γ_4^*